

# Gravitational lensing by Einstein-Born-Infeld black holes

Ernesto F. Eiroa\*

Instituto de Astronomía y Física del Espacio, C.C. 67, Suc. 28, 1428, Buenos Aires, Argentina

May 24, 2019

## Abstract

In this paper, charged black holes in general relativity coupled to Born-Infeld electrodynamics are studied as gravitational lenses. The positions and magnifications of the relativistic images are obtained using the strong deflection limit, and the results are compared with those corresponding to a Reissner-Nordström black hole with the same mass and charge. The model is applied to the Galactic center black hole.

PACS numbers: 98.62.Sb, 04.70.Bw, 04.40.-b

Keywords: gravitational lensing, black hole physics, nonlinear electrodynamics

## 1 Introduction

The study of gravitational deflection of light by a compact object with a photon sphere requires a full strong field treatment, instead of the weak field approximation [1] (i.e., only keeping the first non null term in the expansion of the deflection angle), commonly used for ordinary stars and galaxies. Light rays passing close to the photon sphere will have large deflection angles, resulting in the formation of two infinite sets of faint relativistic images produced by photons that make complete turns (in both directions of rotation) around the black hole before reaching the observer, in addition to the primary and secondary weak field images. In the last few years, there has been a growing interest in strong field lensing situations. Virbhadra and Ellis [2] introduced a lens equation for asymptotically flat spacetimes and made a numerical analysis of lensing due to the black hole situated in the center of the Galaxy, using the Schwarzschild metric. In another article [3], they investigated gravitational lensing by naked singularities. Frittelli, Kling and Newman [4] found an exact lens equation without any reference to a background metric and compared their results with those of Virbhadra and Ellis. A logarithmic approximation was used by several authors [5] to obtain the deflection angle as a function of the impact parameter in Schwarzschild geometry, for light rays passing very close to the photon sphere, in the analysis of strong field situations. This asymptotic approximation is the starting point of an analytical method for strong field lensing, called the strong field limit by Bozza *et al.* [6] or following a suggestion by Perlick [7], the strong deflection limit, which gives the lensing observables in a straightforward way [6]. Eiroa, Romero and Torres [8] extended this method to Reissner-Nordström geometry, and Bozza [9] showed that it can be applied to any static spherically symmetric lens. It was subsequently used by Bhadra [10] to study a charged black hole lens of string theory, by Petters [11] to analyze the relativistic corrections to microlensing effects produced by the Galactic black hole, and by Bozza and Mancini [12] to study the time delay between different relativistic images. All the

---

\*e-mail: eiroa@iafe.uba.ar

above mentioned works treated standard lensing situations, i.e. the lens is placed between the source and the observer. But when the observer is placed between the source and the black hole lens, or the source is situated between the lens and the observer, two infinite sequences of images with deflection angles closer to odd multiples of  $\pi$  are formed, a situation called retrolensing. Holtz and Wheeler [13] considered a black hole retrolens in the galactic bulge with the sun as source, and De Paolis *et al.* [14] analyzed the massive black hole at the Galactic center as retrolens with the bright star S2 as source; in both works, the Schwarzschild metric was used and only the two strongest images were taken into account. Eiroa and Torres [15] studied the general case of a spherically symmetric retrolens, using the strong deflection limit to obtain the positions and magnifications of all images. Bozza and Mancini [16] extended the strong deflection limit to analyze standard lensing, retrolensing and intermediate situations under a unified formalism, and analyzed several stars in the neighborhood of the central Galactic black hole as possible sources. The study of lensing by rotating black holes is more complicated than by spherically symmetric ones. In recent years, some works [17, 18] considered spinning black hole lenses, in most cases restricting their treatment to equatorial or quasi-equatorial lensing scenarios. The complete extension of the strong deflection limit to Kerr geometry was not possible yet, but important advances in this direction were made by Bozza *et al.* [17]. The relativistic images produced by spherically symmetric black holes lenses in the context of braneworld cosmologies were investigated by Eiroa [19] and Whisker [20]. Other related topics about strong field lensing are treated in Refs. [21].

Born and Infeld [22] proposed in 1934 a nonlinear theory of electrodynamics in order to avoid the infinite self energies for charged point particles arising in Maxwell theory. In 1935, Hoffmann [23] joined general relativity with Born–Infeld electrodynamics to obtain a spherically symmetric solution representing the gravitational field of a charged object. These works were nearly forgotten for several decades, until the interest in non linear electrodynamics increased in the context of low energy string theory, in which Born–Infeld type actions appeared [24]. Gibbons and Rasheed showed [25] that Maxwell and Born–Infeld theories are singled out among all electromagnetic theories for having electric-magnetic duality invariance. Hoffmann solution failed to represent a suitable classical field model for the electron, instead it corresponds to that is now called a black hole. Spherically symmetric black holes in non linear electrodynamics coupled to Einstein gravity were studied in recent years by several authors [25, 26]. Plebański [27] found that in Born–Infeld electrodynamics the trajectories of photons in curved spacetimes are not null geodesics of the background metric. Instead, they follow null geodesics of an effective geometry determined by the nonlinearities of the electromagnetic field. Gutierrez *et al.* [28] and Novello *et al.* [29] extended the concept of effective metrics for photons to any nonlinear electromagnetic theory. Bretón [30] analyzed the geodesic structure of Einstein–Born–Infeld black holes for massive particles, photons and gravitons.

In this article the Einstein Born–Infeld black holes are studied as gravitational lenses and the results are compared with those corresponding to Reissner–Nordström geometry. The paper is organized as follows. In Sec. 2, the Einstein–Born–Infeld black holes are reviewed. In Sec. 3, the expression for the deflection angle is found by means of the strong deflection limit. In Sec. 4, the lens equation is used to obtain the positions and magnifications of the relativistic images. In Sec. 5, as a numerical example, the lensing observables for the Galactic center black hole are calculated. Finally, in Sec. 6, a discussion of the results is made.

## 2 Einstein–Born–Infeld black holes

The action of Einstein gravity coupled to Born–Infeld electrodynamics<sup>1</sup> has the form

$$S = \int dx^4 \sqrt{-g} \left( \frac{R}{16\pi} + L_{BI} \right), \quad (1)$$

with

$$L_{BI} = \frac{1}{4\pi b^2} \left( 1 - \sqrt{1 + \frac{1}{2} F_{\sigma\nu} F^{\sigma\nu} b^2 - \frac{1}{4} {}^*F_{\sigma\nu} F^{\sigma\nu} b^4} \right), \quad (2)$$

where  $g$  is the determinant of the metric tensor,  $R$  is the scalar of curvature,  $F_{\sigma\nu} = \partial_\sigma A_\nu - \partial_\nu A_\sigma$  is the electromagnetic tensor,  ${}^*F_{\sigma\nu} = \frac{1}{2} \sqrt{-g} \varepsilon_{\alpha\beta\sigma\nu} F^{\alpha\beta}$  is the Hodge dual of  $F_{\sigma\nu}$  (with  $\varepsilon_{\alpha\beta\sigma\nu}$  the Levi–Civita symbol) and  $b$  is a parameter that indicates how much Born–Infeld and Maxwell electrodynamics differ. In the context of string theory  $b$  is related with the string tension. For  $b \rightarrow 0$  the Einstein–Maxwell action is recovered. The field equations can be obtained by varying the action (1) with respect to the metric  $g_{\sigma\nu}$  and the electromagnetic potential  $A_\nu$ . These field equations have spherically symmetric black hole solutions [25] given by

$$ds^2 = -\psi(r) dt^2 + \psi(r)^{-1} dr^2 + r^2 d\Omega^2, \quad (3)$$

with

$$\psi(r) = 1 - \frac{2M}{r} + \frac{2}{b^2 r} \int_r^\infty \left( \sqrt{x^4 + b^2 Q^2} - x^2 \right) dx, \quad (4)$$

$$D(r) = \frac{Q_E}{r^2}, \quad (5)$$

$$B(r) = Q_M \sin \theta, \quad (6)$$

where  $M$  is the ADM mass,  $Q^2 = Q_E^2 + Q_M^2$  is the sum of the squares of the electric  $Q_E$  and magnetic  $Q_M$  charges,  $B(r)$  and  $D(r)$  are the magnetic and the electric inductions in the local orthonormal frame. In the limit  $b \rightarrow 0$ , the Reissner–Nordström metric is obtained. The metric (3) is also asymptotically Reissner–Nordström for large values of  $r$ . With the units adopted above,  $M$ ,  $Q$  and  $b$  have dimensions of length. The metric function  $\psi(r)$  can be expressed in the form

$$\psi(r) = 1 - \frac{2M}{r} + \frac{2}{3b^2} \left\{ r^2 - \sqrt{r^4 + b^2 Q^2} + \frac{\sqrt{|bQ|^3}}{r} F \left[ \arccos \left( \frac{r^2 - |bQ|}{r^2 + |bQ|} \right), \frac{\sqrt{2}}{2} \right] \right\}, \quad (7)$$

where  $F(\gamma, k)$  is the elliptic integral of the first kind<sup>2</sup>. As in Schwarzschild and Reissner–Nordström cases, the metric (3) has a singularity at  $r = 0$  [30]. The zeros of  $\psi(r)$  determine the position of the horizons, which have to be obtained numerically. For a given value of  $b$ , when the charge is small,  $0 \leq |Q|/M \leq \nu_1$ , the function  $\psi(r)$  has one zero and there is a regular event horizon. For intermediate values of charge,  $\nu_1 < |Q|/M < \nu_2$ ,  $\psi(r)$  has two zeros, so there are, as in the Reissner–Nordström geometry, an inner horizon and an outer regular event horizon. When  $|Q|/M = \nu_2$ , there is one degenerate horizon. Finally, if the values of charge are large,  $|Q|/M > \nu_2$ , the function  $\psi(r)$  has no zeros and a naked singularity is obtained. The values of  $|Q|/M$  where the number of horizons change,  $\nu_1 = (9|b|/M)^{1/3} [F(\pi, \sqrt{2}/2)]^{-2/3}$  and  $\nu_2$ , which should be calculated numerically from the condition

<sup>1</sup>Throughout the paper, units such as  $G = c = 4\pi\epsilon_0 = (4\pi)^{-1}\mu_0 = 1$  are adopted, and the signature of the metric is taken  $(-+++)$ .

<sup>2</sup> $F(\gamma, k) = \int_0^\gamma (1 - k^2 \sin^2 \phi)^{-1/2} d\phi = \int_0^{\sin \gamma} [(1 - z^2)(1 - k^2 z^2)]^{-1/2} dz$  [31]

$\psi(r_h) = \psi'(r_h) = 0$ , are increasing functions of  $|b|/M$ . In the Reissner–Nordström limit ( $b \rightarrow 0$ ) it is easy to see that  $\nu_1 = 0$  and  $\nu_2 = 1$ .

The paths of photons in nonlinear electrodynamics are not null geodesics of the background geometry. Instead, they follow null geodesics of an effective metric [27] generated by the self-interaction of the electromagnetic field, which depends on the particular nonlinear theory considered. In Einstein gravity coupled to Born–Infeld electrodynamics the effective geometry for photons is given by [30]:

$$ds_{eff}^2 = -\omega(r)^{1/2}\psi(r)dt^2 + \omega(r)^{1/2}\psi(r)^{-1}dr^2 + \omega(r)^{-1/2}r^2d\Omega^2, \quad (8)$$

where

$$\omega(r) = 1 + \frac{Q^2b^2}{r^4}. \quad (9)$$

Then, to calculate the deflection angle for photons passing near the black holes considered in the present work, it is necessary to use the effective metric (8) instead of the background metric (3). The horizon structure of the effective metric is the same that of metric (3), but the trajectories of photons are different.

### 3 Deflection angle

For a spherically symmetric black hole with a metric of the form

$$ds^2 = -f(r)dt^2 + g(r)dr^2 + h(r)d\Omega^2, \quad (10)$$

the radius of the event horizon  $r_h$  is given by the greatest positive root of the equation  $f(r) = 0$ , and the radius of the photon sphere  $r_{ps}$  by the greatest positive solution of the equation  $f(r)h'(r) = f'(r)h(r)$ , where the prime means the derivative respect to the radial coordinate  $r$ . The deflection angle for a photon coming from infinite is given by [32]

$$\alpha(r_0) = I(r_0) - \pi, \quad (11)$$

where  $r_0$  is the closest approach distance and

$$I(r_0) = \int_{r_0}^{\infty} 2 \left[ \frac{g(r)}{h(r)} \right]^{1/2} \left[ \frac{h(r)f(r_0)}{h(r_0)f(r)} - 1 \right]^{-1/2} dr. \quad (12)$$

For the effective metric (8) the integral is

$$I(r_0) = 2 \int_{r_0}^{\infty} \frac{r_0\omega(r)}{r\sqrt{\omega(r_0)\psi(r_0)r^2 - r_0^2\omega(r)\psi(r)}} dr, \quad (13)$$

thus, defining  $\chi(r) = \omega(r)\psi(r)$  and making the substitution  $z = r_0/r$ , it takes the form

$$I(r_0) = 2 \int_0^1 \frac{\omega(r_0/z)}{\sqrt{\chi(r_0) - \chi(r_0/z)z^2}} dz. \quad (14)$$

The functions inside the integral  $\omega(r_0/z)$  and  $\chi(r_0) - \chi(r_0/z)z^2$  can be expanded in powers of  $1 - z$ :

$$\omega(r_0/z) = 1 + \frac{Q^2b^2}{r_0^4} - 4\frac{Q^2b^2}{r_0^4}(1 - z) + O(1 - z)^2, \quad (15)$$

$$\chi(r_0) - \chi(r_0/z)z^2 = \gamma_1(r_0)(1-z) + \gamma_2(r_0)(1-z)^2 + O(1-z)^3, \quad (16)$$

where  $\gamma_1(r_0) = 2\chi(r_0) - r_0\chi'(r_0)$  and  $\gamma_2(r_0) = -\chi(r_0) + r_0\chi'(r_0) - (1/2)r_0^2\chi''(r_0)$ . For the effective metric (8) the photon sphere radius  $r_{ps}$  is given by the greatest positive solution of the equation  $2\chi(r) - r\chi'(r) = 0$ , which should be solved numerically. When  $r_0 > r_{ps}$ ,  $\gamma_1(r_0) \neq 0$  and the leading term inside the integral in Eq. (14) is proportional to  $1/\sqrt{(1-z)}$ , so it converges. As  $\gamma_1(r_{ps}) = 0$ , for  $r_0 = r_{ps}$  the leading term goes as  $1/(1-z)$  and the integral has a logarithmic divergence. Then, following Ref. [9], it is convenient to separate  $I(r_0)$  as a sum of two parts:

$$I(r_0) = I_D(r_0) + I_R(r_0), \quad (17)$$

with

$$I_D(r_0) = 2 \int_0^1 \frac{r_0^4 + Q^2b^2}{r_0^4 \sqrt{\gamma_1(r_0)(1-z) + \gamma_2(r_0)(1-z)^2}} dz, \quad (18)$$

and

$$I_R(r_0) = 2 \int_0^1 \left[ \frac{\omega(r_0/z)}{\sqrt{\chi(r_0) - \chi(r_0/z)z^2}} - \frac{r_0^4 + Q^2b^2}{r_0^4 \sqrt{\gamma_1(r_0)(1-z) + \gamma_2(r_0)(1-z)^2}} \right] dz. \quad (19)$$

The integral  $I_D(r_0)$ , which diverges for  $r_0 = r_{ps}$ , can be calculated exactly to give

$$I_D(r_0) = -\frac{2(r_0^4 + Q^2b^2)}{r_0^4 \sqrt{\gamma_2(r_0)}} \ln \frac{\gamma_1(r_0)}{[\sqrt{\gamma_1(r_0) + \gamma_2(r_0)} + \sqrt{\gamma_2(r_0)}]^2}, \quad (20)$$

and for  $r_0$  close to  $r_{ps}$  it takes the form

$$I_D(r_0) = -\frac{\sqrt{8}(r_{ps}^4 + Q^2b^2)}{r_{ps}^4 \sqrt{2\chi(r_{ps}) - r_{ps}^2\chi''(r_{ps})}} \left[ \ln \left( \frac{r_0}{r_{ps}} - 1 \right) - \ln 2 \right] + O(r_0 - r_{ps}), \quad (21)$$

where it was used that  $2\chi(r_{ps}) - r_{ps}\chi'(r_{ps}) = 0$ . The integral  $I_R(r_0)$  is the original integral  $I(r_0)$  with the divergence subtracted, so it converges when  $r_0 = r_{ps}$ , and it can be replaced by  $I_R(r_0) = I_R(r_{ps}) + O(r_0 - r_{ps})$ .

The deflection angle, which diverges for  $r_0 = r_{ps}$ , is thus given in the strong deflection limit by

$$\alpha(r_0) = -a_1 \ln \left( \frac{r_0}{r_{ps}} - 1 \right) + a_2 + O(r_0 - r_{ps}), \quad (22)$$

where

$$a_1 = \frac{\sqrt{8}(r_{ps}^4 + Q^2b^2)}{r_{ps}^4 \sqrt{2\chi(r_{ps}) - r_{ps}^2\chi''(r_{ps})}}, \quad (23)$$

and

$$a_2 = -\pi + a_D + a_R, \quad (24)$$

with

$$a_D = a_1 \ln 2, \quad (25)$$

and

$$a_R = I_R(r_{ps}) = 2 \int_0^1 \left[ \frac{\omega(r_{ps}/z)}{\sqrt{\chi(r_{ps}) - \chi(r_{ps}/z)z^2}} - \frac{\sqrt{2}(r_{ps}^4 + Q^2b^2)}{(1-z)r_{ps}^4 \sqrt{2\chi(r_{ps}) - r_{ps}^2\chi''(r_{ps})}} \right] dz. \quad (26)$$

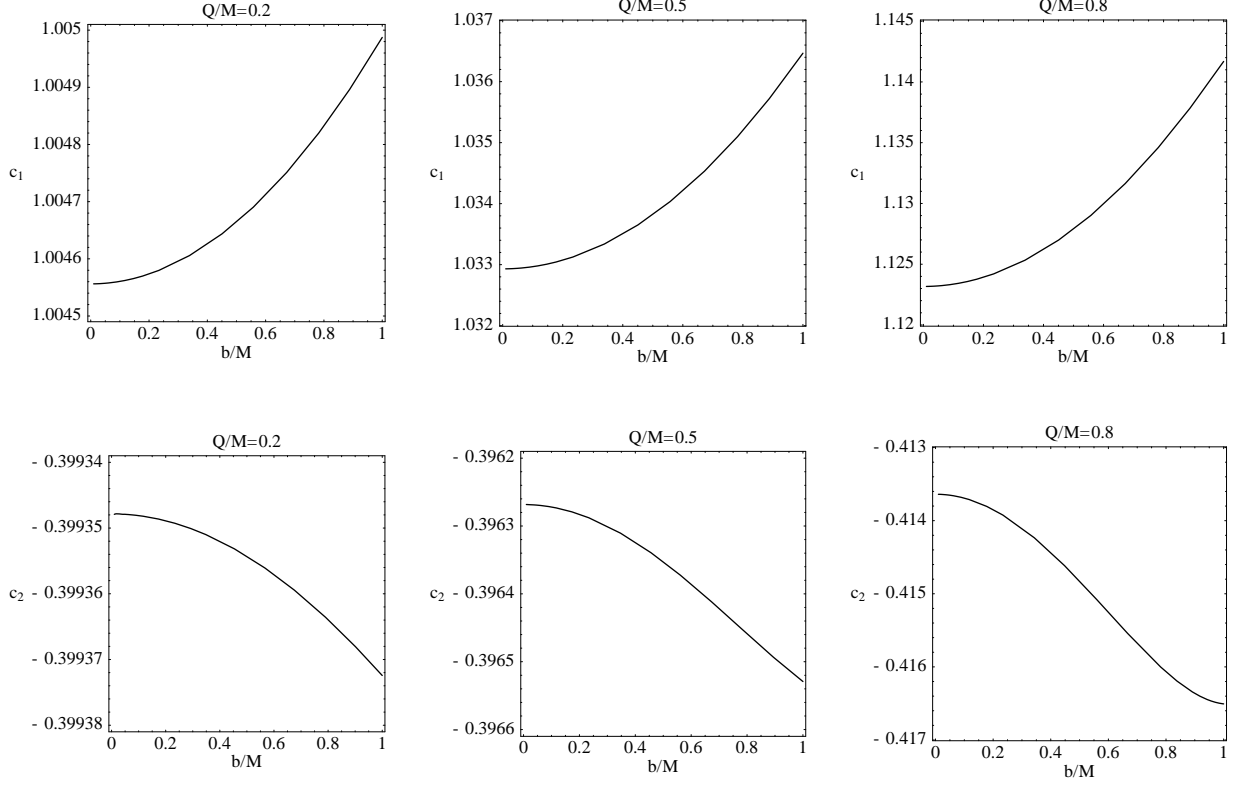


Figure 1: The strong deflection limit coefficients  $c_1$  (upper panel) and  $c_2$  (lower panel) as functions of the Born–Infeld parameter  $b$  for different values of the charge  $Q$ . When  $b = 0$  the coefficients corresponding to Reissner–Nordström black holes are obtained. The Schwarzschild values are  $c_1^{Schw} = 1$  and  $c_2^{Schw} = \ln[216(7 - 4\sqrt{3})] - \pi \approx -0.40023$ .

As it happens in the Reissner–Nordström case, when  $Q \neq 0$  it is not possible to calculate this integral in an exact form. It can be obtained approximately, by means of a numerical treatment or making a power expansion in  $Q$ . The impact parameter  $u$ , defined as the perpendicular distance from the black hole to the asymptotic path at infinite, is more easily related with the lensing angles than the closest approach distance  $r_0$ . Following Ref. [32],  $u = [h(r_0)/f(r_0)]^{1/2}$ , which in our case gives  $u = r_0/\sqrt{\chi(r_0)}$ . Making a second order Taylor expansion around  $r_0 = r_{ps}$ , it takes the form

$$u = u_{ps} + \frac{2\chi(r_{ps}) - r_{ps}^2\chi''(r_{ps})}{4r_{ps}[\chi(r_{ps})]^{3/2}}(r_0 - r_{ps})^2 + O(r_0 - r_{ps})^3, \quad (27)$$

where  $u_{ps} = r_{ps}/\sqrt{\chi(r_{ps})}$  is the critical impact parameter. Inverting Eq. (27):

$$\frac{r_0}{r_{ps}} - 1 = \left[ \frac{2\chi(r_{ps}) - r_{ps}^2\chi''(r_{ps})}{4\chi(r_{ps})} \right]^{-1/2} \left( \frac{u}{u_{ps}} - 1 \right)^{1/2}. \quad (28)$$

Then the deflection angle can be obtained as a function of the impact parameter  $u$ :

$$\alpha(u) = -c_1 \ln \left( \frac{u}{u_{ps}} - 1 \right) + c_2 + O(u - u_{ps}), \quad (29)$$

with  $c_1 = a_1/2$  and

$$c_2 = \frac{a_1}{2} \ln \frac{2\chi(r_{ps}) - r_{ps}^2 \chi''(r_{ps})}{4\chi(r_{ps})} + a_2. \quad (30)$$

Eq. (29) represents the strong deflection limit approximation of the deflection angle as a function of the impact parameter. Photons with an impact parameter slightly greater than the critical value  $u_{ps}$  will spiral out, eventually reaching the observer after one or more turns around the black hole. In this case, the strong deflection limit gives a good approximation for the deflection angle. Those photons whose impact parameter is smaller than  $u_{ps}$  will spiral into the black hole, not reaching any observer outside the photon sphere. The coefficients  $c_1$  and  $c_2$  (obtained numerically) are plotted as functions of the Born–Infeld parameter  $b$  in Fig. 1. For a given non null value of charge,  $c_1$  increases and  $c_2$  decreases (becomes more negative) with  $b$ , thus the Einstein–Born–Infeld black holes have larger  $c_1$  and smaller  $c_2$  than their Reissner–Nordström counterparts with the same charge. The differences between these geometries grow as  $|Q|$  increases. When the charge is zero, the Schwarzschild geometry is recovered, with the strong field limit coefficients given by  $c_1^{Schw} = 1$  and  $c_2^{Schw} = \ln[216(7 - 4\sqrt{3})] - \pi \approx 0.40023$ .

## 4 Positions and magnifications of the relativistic images

The lens geometry consists of a point source of light (s), a black hole, which it is called the lens (l), and the observer (o), with three possible configurations of them. The configuration where the lens between the observer and the source is named standard lensing (SL). Those corresponding to the source between the observer and the lens (RLI), or the observer between the source and the lens (RLII) are called retrolensing. The line joining the observer and the lens define the optical axis and the background space-time is asymptotically flat, with both the observer and the source in the flat region. The angular positions, seen from the observer, of the source and the images are, respectively,  $\beta$  (taken positive without losing generality) and  $\theta$ . The observer-source ( $d_{os}$ ), observer-lens ( $d_{ol}$ ) and the lens-source ( $d_{ls}$ ) distances (measured along the optical axis) are taken much greater than the horizon radius. The lens equation is given by

$$\tan \beta = \tan \theta - c_3 [\tan(\alpha - \theta) + \tan \theta], \quad (31)$$

where  $c_3 = d_{ls}/d_{os}$  (SL) [2],  $c_3 = d_{os}/d_{ol}$  (RLI) [15] or  $c_3 = d_{os}/d_{ls}$  (RLII) [19], depending on the configuration considered. The lensing effects are more important when the objects are highly aligned, so the analysis will be restricted to this case<sup>3</sup>, in which the angles  $\beta$  and  $\theta$  are small, and  $\alpha$  is close to an even multiple of  $\pi$  for standard lensing or to an odd multiple of  $\pi$  for retrolensing. In the standard lensing case, when  $\beta \neq 0$  two weak field primary and secondary images, which will be not considered here, and two infinite sets of point relativistic images are formed. The first set of relativistic images have a deflection angle that can be written as  $\alpha = 2n\pi + \Delta\alpha_n$ , with  $n \in \mathbb{N}$  and  $0 < \Delta\alpha_n \ll 1$ . Then, the lens equation can be simplified:

$$\beta = \theta - c_3 \Delta\alpha_n. \quad (32)$$

To obtain the other set of images, it should be taken  $\alpha = -2n\pi - \Delta\alpha_n$ , so  $\Delta\alpha_n$  must be replaced by  $-\Delta\alpha_n$  in Eq. (32). From the lens geometry it is easy to see that  $u = d_{ol} \sin \theta$ , which can be approximated to first order in  $\theta$  by  $u = d_{ol} \theta$ , so the deflection angle given by Eq. (29) can be written as a function of  $\theta$ :

$$\alpha(\theta) = -c_1 \ln \left( \frac{d_{ol} \theta}{u_{ps}} - 1 \right) + c_2. \quad (33)$$

---

<sup>3</sup>for a unified treatment of standard lensing, retrolensing and intermediate situations in the strong deflection limit, see Ref. [16]

Then, inverting Eq. (33) to obtain  $\theta(\alpha)$

$$\theta(\alpha) = \frac{u_{ps}}{d_{ol}} \left[ 1 + e^{(c_2 - \alpha)/c_1} \right], \quad (34)$$

and making a first order Taylor expansion around  $\alpha = 2n\pi$ , the angular position of the  $n$ -th image is

$$\theta_n = \theta_n^0 - \zeta_n \Delta\alpha_n, \quad (35)$$

with

$$\theta_n^0 = \frac{u_{ps}}{d_{ol}} \left[ 1 + e^{(c_2 - 2n\pi)/c_1} \right], \quad (36)$$

and

$$\zeta_n = \frac{u_{ps}}{c_1 d_{ol}} e^{(c_2 - 2n\pi)/c_1}. \quad (37)$$

From Eq. (32),  $\Delta\alpha_n = (\theta_n - \beta)/c_3$ , so replacing it in Eq. (35) gives

$$\theta_n = \theta_n^0 - \frac{\zeta_n}{c_3} (\theta_n - \beta), \quad (38)$$

which can be expressed in the form

$$\theta_n = \left( 1 + \frac{\zeta_n}{c_3} \right)^{-1} \left( \theta_n^0 + \frac{\zeta_n}{c_3} \beta \right), \quad (39)$$

then, using that  $0 < \zeta_n/c_3 \ll 1$  and keeping only the first order term in  $\zeta_n/c_3$ , the angular positions of the images can be approximated by

$$\theta_n = \theta_n^0 + \frac{\zeta_n}{c_3} (\beta - \theta_n^0). \quad (40)$$

The second term in Eq. (40) is a small correction on  $\theta_n^0$ , so all images lie very close to  $\theta_n^0$ . With a similar treatment, the other set of relativistic images have angular positions

$$\theta_n = -\theta_n^0 + \frac{\zeta_n}{c_3} (\beta + \theta_n^0). \quad (41)$$

In the case of perfect alignment ( $\beta = 0$ ), instead of point images an infinite sequence of concentric rings is obtained, with angular radius

$$\theta_n^E = \left( 1 - \frac{\zeta_n}{c_3} \right) \theta_n^0, \quad (42)$$

which are usually called Einstein rings.

It is a well known result that gravitational lensing conserves surface brightness [1], so the ratio of the solid angles subtended by the image and the source gives the magnification of the  $n$ -th image:

$$\mu_n = \left| \frac{\sin \beta}{\sin \theta_n} \frac{d\beta}{d\theta_n} \right|^{-1} \approx \left| \frac{\beta}{\theta_n} \frac{d\beta}{d\theta_n} \right|^{-1}, \quad (43)$$

which, using Eq. (40), leads to

$$\mu_n = \frac{1}{\beta} \left[ \theta_n^0 + \frac{\zeta_n}{c_3} (\beta - \theta_n^0) \right] \frac{\zeta_n}{c_3}, \quad (44)$$

that can be approximated to first order in  $\zeta_n/c_3$  by

$$\mu_n = \frac{1}{\beta} \frac{\theta_n^0 \zeta_n}{c_3}. \quad (45)$$

The same expression is obtained for the other set of relativistic images. The first image is the brightest one, and the magnifications decrease exponentially with  $n$ . For retrolensing, the same equations for the positions and magnifications of the relativistic images apply, with  $2n$  replaced by  $2n - 1$  in the expressions of  $\theta_n^0$  and  $\zeta_n$ . The magnifications of the images are greater in retrolensing configurations. In all cases, the magnifications are proportional to  $(u_{ps}/d_{ol})^2$ , which is a very small factor. Then, the relativistic images are very faint, unless  $\beta$  has values close to zero, i.e. nearly perfect alignment. For  $\beta = 0$ , the magnification becomes infinite, and the point source approximation breaks down, so an extended source analysis is needed. The magnification of the images for an extended source is obtained by integrating over its luminosity profile:

$$\mu_n^{ext} = \frac{\iint_S \mathcal{I} \mu_p dS}{\iint_S \mathcal{I} dS}, \quad (46)$$

where  $\mathcal{I}$  is the surface intensity distribution of the source and  $\mu_p$  is the magnification corresponding to each point of the source. When the source is an uniform disk  $D(\beta_c, \beta_s)$ , with angular radius  $\beta_s$  and centered in  $\beta_c$  (taken positive), Eq. (46) takes the form

$$\mu_n^{ext} = \frac{\iint_{D(\beta_c, \beta_s)} \mu_p dS}{\pi \beta_s^2}. \quad (47)$$

So, using Eq. (45), the magnification of the relativistic  $n$ -th image for an extended uniform source is

$$\mu_n^{ext} = \frac{I}{\pi \beta_s^2} \frac{\theta_n^0 \zeta_n}{c_3}, \quad (48)$$

with

$$I = 2 \left[ (\beta_s + \beta_c) E \left( \frac{2\sqrt{\beta_s \beta_c}}{\beta_s + \beta_c} \right) + (\beta_s - \beta_c) K \left( \frac{2\sqrt{\beta_s \beta_c}}{\beta_s + \beta_c} \right) \right], \quad (49)$$

where  $K(k)$  and  $E(k)$  are respectively, complete elliptic integrals of the first<sup>4</sup> and second<sup>5</sup> kind. Finite magnifications are always obtained from Eq. (48), even in the case of complete alignment.

The total magnification, taking into account both sets of images, is  $\mu = 2 \sum_{n=1}^{\infty} \mu_n$  which for a point source, using Eqs. (36), (37) and (45), gives

$$\mu = \frac{1}{\beta} \frac{2u_{ps}^2}{d_{ol}^2 c_1 c_3} \frac{e^{c_2/c_1} (1 + e^{c_2/c_1} + e^{2\pi/c_1})}{e^{4\pi/c_1} - 1} \quad (50)$$

for standard lensing, and

$$\mu = \frac{1}{\beta} \frac{2u_{ps}^2}{d_{ol}^2 c_1 c_3} \frac{e^{(c_2+\pi)/c_1} [1 + e^{(c_2+\pi)/c_1} + e^{2\pi/c_1}]}{e^{4\pi/c_1} - 1} \quad (51)$$

---

<sup>4</sup> $K(k) = \int_0^{\pi/2} (1 - k^2 \sin^2 \phi)^{-1/2} d\phi = \int_0^1 [(1 - z^2)(1 - k^2 z^2)]^{-1/2} dz$  [31]

<sup>5</sup> $E(k) = \int_0^{\pi/2} (1 - k^2 \sin^2 \phi)^{1/2} d\phi = \int_0^1 (1 - z^2)^{-1/2} (1 - k^2 z^2)^{1/2} dz$  [31]

for retrolensing. When the source is extended, the total magnification is given by

$$\mu^{ext} = \frac{I}{\pi\beta_s^2} \frac{2u_{ps}^2}{d_{ol}^2 c_1 c_3} \frac{e^{c_2/c_1} (1 + e^{c_2/c_1} + e^{2\pi/c_1})}{e^{4\pi/c_1} - 1} \quad (52)$$

for standard lensing, and

$$\mu^{ext} = \frac{I}{\pi\beta_s^2} \frac{2u_{ps}^2}{d_{ol}^2 c_1 c_3} \frac{e^{(c_2+\pi)/c_1} [1 + e^{(c_2+\pi)/c_1} + e^{2\pi/c_1}]}{e^{4\pi/c_1} - 1} \quad (53)$$

for retrolensing.

## 5 Application to the Galactic center black hole

The first image, with angular position  $\theta_1$ , is the outermost one, and the others approach to the limiting value  $\theta_\infty = u_{ps}/d_{ol}$  as  $n$  increases. The lensing observables defined by Bozza [9]:

$$s = \theta_1 - \theta_\infty \quad (54)$$

and

$$r = \frac{\mu_1}{\sum_{n=2}^{\infty} \mu_n} \quad (55)$$

are useful when the outermost image can be resolved from the rest. The observable  $s$  represents the angular separation between the first image and the limiting value of the succession of images, and  $r$  is the ratio between the flux of the first image and the sum of the fluxes of the other images. For high alignment, they can be approximated by

$$s_{SL} = \theta_\infty e^{(c_2-2\pi)/c_1}, \quad (56)$$

$$r_{SL} = e^{2\pi/c_1} + e^{c_2/c_1} - 1, \quad (57)$$

for standard lensing, and by

$$s_{RL} = \theta_\infty e^{(c_2-\pi)/c_1}, \quad (58)$$

$$r_{RL} = e^{2\pi/c_1} + e^{(c_2+\pi)/c_1} - 1, \quad (59)$$

for retrolensing. The strong deflection limit coefficients  $c_1$  and  $c_2$  can be obtained by measuring  $\theta_\infty$ ,  $s$  and  $r$  and inverting Eqs. (56) and (57) (SL) or Eqs. (58) and (59) (RL). Then, their values can be compared with those predicted by the theoretical models to identify the nature of the black hole lens.

To give a numerical example, the Galactic center black hole is considered as gravitational lens. The black hole mass is  $M = 3.6 \times 10^6 M_\odot$  [33] and its distance from the Earth is 7.6 Kpcs [33]. The results corresponding to the observables defined above are shown in Figs. 2 and 3. The limiting angular position  $\theta_\infty$  is about  $24 \mu\text{as}$  and the outermost image is about  $0.03 - 0.06 \mu\text{as}$  from  $\theta_\infty$  for standard lensing and  $0.7 - 0.9 \mu\text{as}$  for retrolensing. For a given charge  $Q$ , the angle  $\theta_\infty$  decreases with  $b$ , indicating that the images are closer to the optical axis than for Reissner–Nordström geometry. The quantity  $s$ , instead, is an increasing function of  $b$ , for both standard lensing and retrolensing, so the images have a greater separation between them than in the Reissner–Nordström case. The decreasing

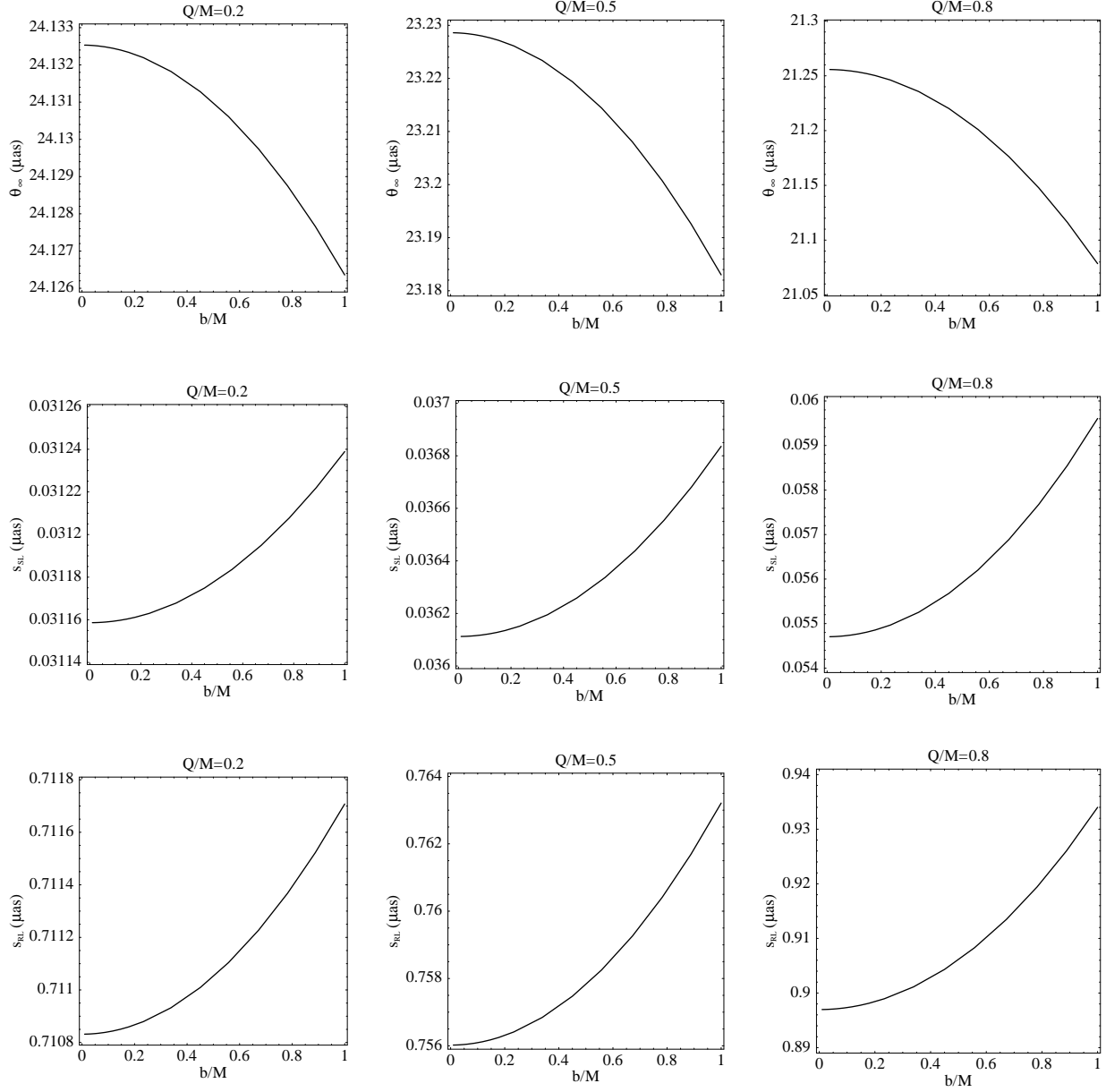


Figure 2: Gravitational lensing by the Galactic center black hole. The values in microarcseconds ( $\mu\text{as}$ ) of  $\theta_\infty$  (upper panel),  $s_{SL}$  (center) and  $s_{RL}$  (lower panel) are plotted as functions of the Born–Infeld parameter  $b$  for different values of the charge  $Q$ . When  $b = 0$  the results corresponding to Reissner–Nordström geometry are obtained. The Schwarzschild black hole values are  $\theta_\infty^{Schw} = 24.296 \mu\text{as}$ ,  $s_{SL}^{Schw} = 0.03041 \mu\text{as}$  and  $s_{RL}^{Schw} = 0.7036 \mu\text{as}$ .

values of the observable  $r$  with  $b$ , in both lensing configurations, indicates that the first relativistic image is less prominent with respect to the others than in Einstein–Maxwell gravity. It is important to remark that the differences between Einstein–Born–Infeld and Reissner–Nordström geometries are very small and they grow by increasing the absolute value of the charge. The relativistic images are highly demagnified, so a bright source with high alignment and instruments with great sensitivity are

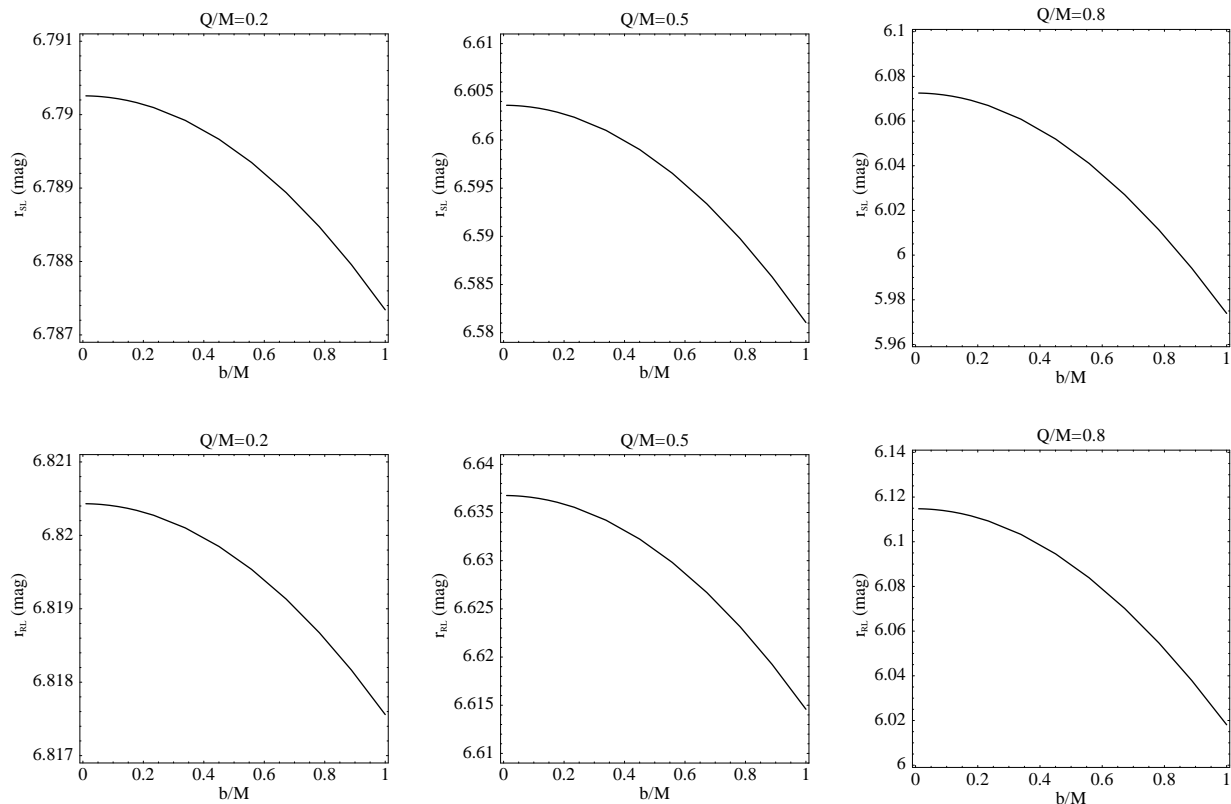


Figure 3: Gravitational lensing by the Galactic center black hole. The values in magnitudes of  $r_{SL}(\text{mag}) = 2.5 \log r_{SL}$  (upper panel) and  $r_{RL}(\text{mag}) = 2.5 \log r_{RL}$  (lower panel) are plotted as functions of the Born–Infeld parameter  $b$  for different values of the charge  $Q$ . When  $b = 0$  the results corresponding to Reissner–Nordström black holes are obtained. The values for Schwarzschild geometry are  $r_{SL}^{Schw}(\text{mag}) \approx 6.8212$  and  $r_{RL}^{Schw}(\text{mag}) \approx 6.8509$ .

required in order to observe them. Angular resolutions of less than  $1 \mu\text{as}$  are also needed to separate the first image from the others. As it was shown by Eiroa and Torres [15], retrolensing images would be easier to detect than the standard lensing ones.

## 6 Conclusions

In this work, Einstein–Born–Infeld black holes were studied as gravitational lenses. In nonlinear electrodynamics, as a consequence of the self interaction of the electromagnetic field, photons follow null geodesics of an effective metric instead of those corresponding to the background geometry. The strong deflection limit coefficients  $c_1$  and  $c_2$  were numerically obtained from the effective metric, and they were subsequently used to find analytically the positions and magnifications of the relativistic images. The model was applied to the black hole in the Galactic center. For a given value of charge, the innermost images are closer to the optical axis and the separations between the images grow as the Born–Infeld parameter  $b$  increases. The images are highly demagnified and the outermost one is less prominent with respect to the others for increasing values of  $b$ . The differences with Reissner–Nordström black hole lenses are very small and become more important for large values of charge. The gravitational lensing effects could be in principle used to discriminate between different black

hole models, but the tiny differences between Einstein–Maxwell and Einstein–Born–Infeld spherically symmetric spacetimes will be extremely difficult to detect. The astronomical observation of these effects is beyond present technical capabilities and it will be a challenge for future facilities. Detailed discussions about the observational prospects of strong deflection lensing are given in Refs. [16, 34].

## Acknowledgments

The author would like to thank Rafael Ferraro and Santiago E. Perez Bergliaffa for helpful discussions. This work has been partially supported by UBA (UBACYT X-103).

## References

- [1] P. Schneider, J. Ehlers, and E.E. Falco, *Gravitational Lenses* (Springer-Verlag, Berlin, 1992).
- [2] K.S. Virbhadra, and G.F.R. Ellis, *Phys. Rev. D* **62**, 084003 (2000).
- [3] K.S. Virbhadra, and G.F.R. Ellis, *Phys. Rev. D* **65**, 103004 (2002).
- [4] S. Frittelli, T.P. Kling, and E.T. Newman, *Phys. Rev. D* **61**, 064021 (2000).
- [5] C. Darwin, *Proc. Roy. Soc London A* **249**, 180 (1959); J.-P. Luminet, *Astron. Astrophys.* **75**, 228 (1979); S. Chandrasekhar, *The Mathematical Theory of Black Holes* (Oxford University Press, Oxford, 1983); H.C. Ohanian, *Am. J. Phys.* **55**, 428 (1987).
- [6] V. Bozza, S. Capozziello, G. Iovane, and G. Scarpetta, *Gen. Relativ. Gravit.* **33**, 1535 (2001).
- [7] V. Perlick, *Phys. Rev. D* **69**, 064017 (2004).
- [8] E.F. Eiroa, G.E. Romero, and D.F. Torres, *Phys. Rev. D* **66**, 024010 (2002).
- [9] V. Bozza, *Phys. Rev. D* **66**, 103001 (2002).
- [10] A. Bhadra, *Phys. Rev. D* **67**, 103009 (2003).
- [11] A.O. Petters, *Mon. Not. R. Astron. Soc.* **338**, 457 (2003).
- [12] V. Bozza, and L. Mancini, *Gen. Relativ. Gravit.* **36**, 435 (2004).
- [13] D.E. Holtz and J.A. Wheeler, *Astrophys. J.* **578**, 330 (2002).
- [14] F. De Paolis, A. Geralico, G. Ingrosso, and A.A. Nucita, *Astron. Astrophys.* **409**, 809 (2003).
- [15] E.F. Eiroa and D.F. Torres, *Phys. Rev. D* **69**, 063004 (2004).
- [16] V. Bozza and L. Mancini, *Astrophys. J.* **611**, 1045 (2004); V. Bozza and L. Mancini, *Astrophys. J.* **627**, 790 (2005).
- [17] V. Bozza, *Phys. Rev. D* **67**, 103006 (2003); V. Bozza, F. De Luca, G. Scarpetta and M. Sereno, *Phys. Rev. D* **72**, 083003 (2005).
- [18] F. De Paolis, A. Geralico, G. Ingrosso, A.A. Nucita, and A. Qadir, *Astron. Astrophys.* **415**, 1 (2004); S.E. Vazquez and E.P. Esteban, *Nuovo Cimento B* **119**, 489 (2004); A.F. Zakharov, A.A. Nucita, F. De Paolis, and G. Ingrosso, astro-ph/0411511.

- [19] E.F. Eiroa, Phys. Rev. D **71**, 083010 (2005).
- [20] R. Whisker, Phys. Rev. D **71**, 064004 (2005).
- [21] R.J. Nemiroff, Am. J. Phys. **61**, 619 (1993); S. Frittelli and E.T. Newman, Phys. Rev. D **59**, 124001 (1999); M.P. Dabrowski and F.E. Schunck, Astrophys. J. **535**, 316 (2000); C.M. Claudel, K.S. Virbhadra, and G.F.R. Ellis, J. Math. Phys. **42**, 818 (2001); V. Perlick, Commun. Math. Phys. **220**, 403 (2001); S. Frittelli and E.T. Newman, Phys. Rev. D **65**, 123006 (2002); S. Frittelli, T.P. Kling, and E.T. Newman, Phys. Rev. D **65**, 123007 (2002).
- [22] M. Born and L. Infeld, Proc. Roy. Soc. **A144**, 425 (1934).
- [23] B. Hoffmann, Phys. Rev. **47**, 877 (1935).
- [24] E.S. Fradkin and A.A. Tseytlin, Phys. Lett. B **163**, 123 (1985); E. Bergshoeff, E. Sezgin, C.N. Pope, and P.K. Townsend, Phys. Lett. B **188**, 70 (1987); R.R. Metsaev, M.A. Rahmanov, and A.A. Tseytlin, Phys. Lett. B **193**, 207 (1987); A.A. Tseytlin, Nucl. Phys. B **501**, 41 (1997); D. Brecher and M.J. Perry, Nucl. Phys. B **527**, 121 (1998).
- [25] G.W. Gibbons and D.A. Rasheed, Nucl. Phys. B **454**, 185 (1995).
- [26] A. García, H. Salazar and J. F. Plebański, Nuovo Cimento B **84**, 65 (1984); D.L. Wiltshire, Phys. Rev. D **38**, 2445 (1988); H.P. Oliveira, Class. Quantum Grav. **11**, 1469 (1994); E. Ayón-Beato and A. García, Phys. Rev. Lett. **80**, 5056 (1998); M. Novello, S.E. Perez Bergliaffa and J.M. Salim, Class. Quantum Grav. **17**, 3821 (2000); K.A. Bronnikov, Phys. Rev. D **63**, 044005 (2001); A. Burinskii and S.R. Hildebrandt, Phys. Rev. D **65**, 104017 (2002); S. Fernando and D. Krug, Gen. Relat. Grav. **35**, 129 (2002); T. Kumar Dey, Phys. Lett. B **595**, 484 (2004).
- [27] J.F. Plebański, *Lectures on Nonlinear Electrodynamics* (Nordita, Copenhagen, 1970).
- [28] S.A. Gutierrez, A.L. Dudley, and J.F. Plebański, J. Math. Phys. **22**, 2835 (1981).
- [29] M. Novello, V.A. De Lorenci, J.M. Salim and R. Klippert, Phys. Rev. D **61**, 045001 (2000).
- [30] N. Bretón, Class. Quantum Grav. **19**, 601 (2002).
- [31] I.S. Gradshteyn and I.M. Ryzhik, *Table of Integrals, Series and Products*, 5th ed., edited by A. Jeffrey (Academic Press, San Diego, 1994).
- [32] S. Weinberg, *Gravitation and Cosmology: Principles and Applications of the General Theory of Relativity* (Wiley, New York, 1972).
- [33] F. Eisenhauer *et al.*, Astrophys. J. **628**, 246 (2005).
- [34] A.F. Zakharov, A.A. Nucita, F. De Paolis, and G. Ingrosso, New Astron. **10**, 479 (2005); A.F. Zakharov, F. De Paolis, G. Ingrosso, and A.A. Nucita, Astron. Astrophys. **442**, 795 (2005).